

Land applications of SAR remote sensing

Thuy Le Toan

Centre d'Etudes Spatiales de la Biosphère
CNES-CNRS-Université Paul Sabatier- IRD
Toulouse, France



Why observe the land with SAR?

All weather imaging has particular benefits for

- ⇒ Agriculture monitoring
- ⇒ Forest monitoring
- ⇒ Snow and ice studies

Sensitivity to surface roughness

- ⇒ Geological mapping
- ⇒ Topography mapping

Sensitivity to dielectric properties

- ⇒ Soil moisture monitoring
- ⇒ Biomass mapping



Mapping land surfaces and monitoring of bio-geophysical parameters for land applications

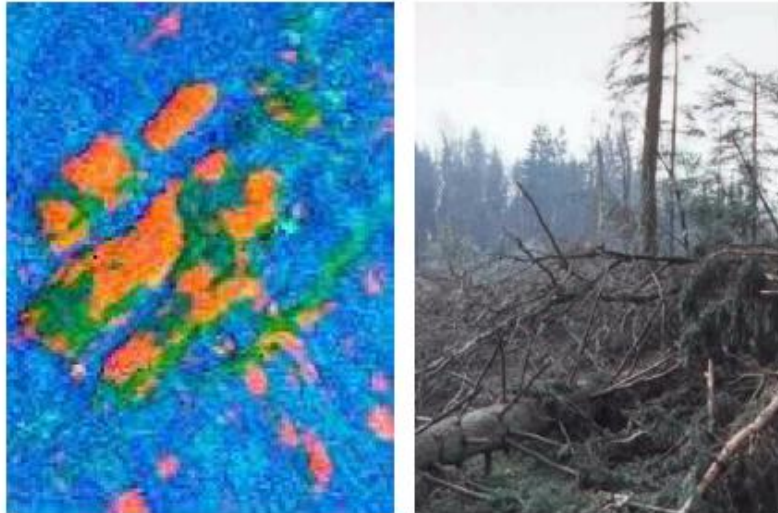


Hazard mapping



Hazard mapping : forest storm damage

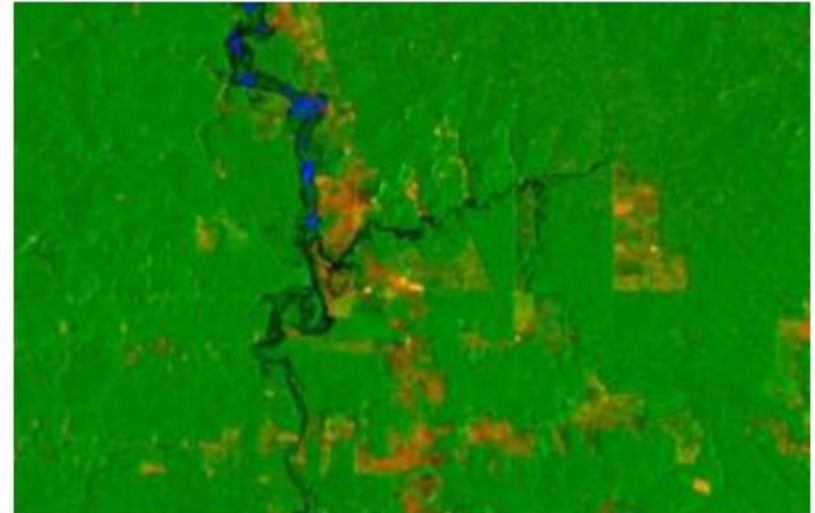
in January 2000, the last acquisition series of ERS tandem



Hazard mapping

Forest damage (orange areas) caused by storm "Lothar" in Dec. 1999, as mapped with multi-temporal ERS SAR interferometry.

Raw data courtesy of ESA. Processing by GAMMA.



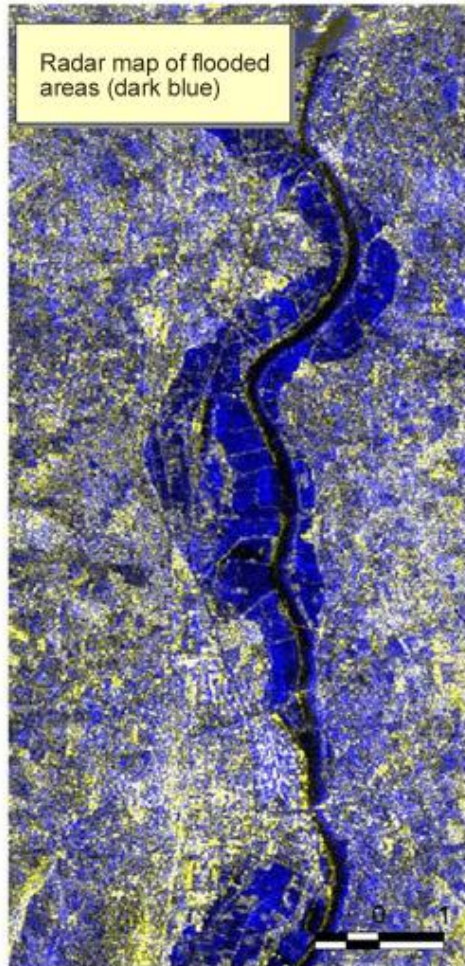
ERS Coherence Product

ERS Tandem coherence (red), backscattering (green), and backscatter change (blue) used to characterize deforestation area.

Raw data courtesy of ESA. Processing by GAMMA.



Situation between Belleville and Villefranche on 27/03/01

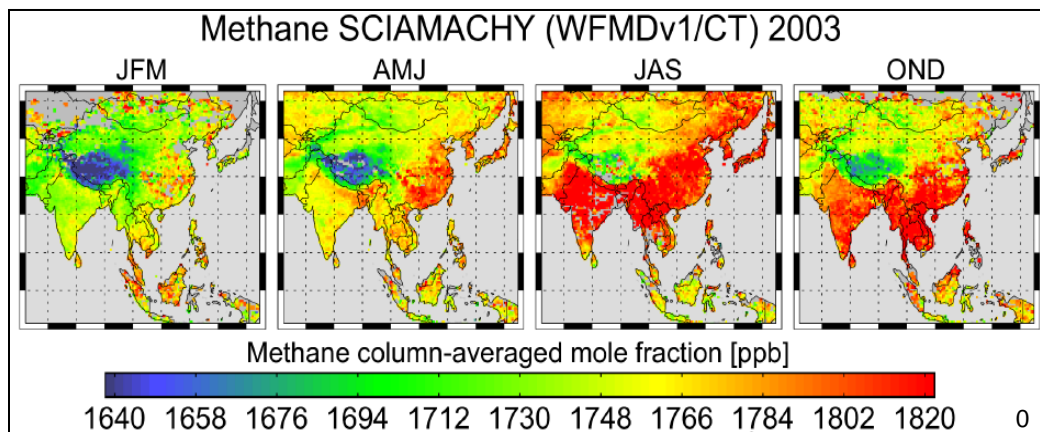


Rice monitoring



Rice: a local interest and a global concern

■ Impact of rice on climatic change

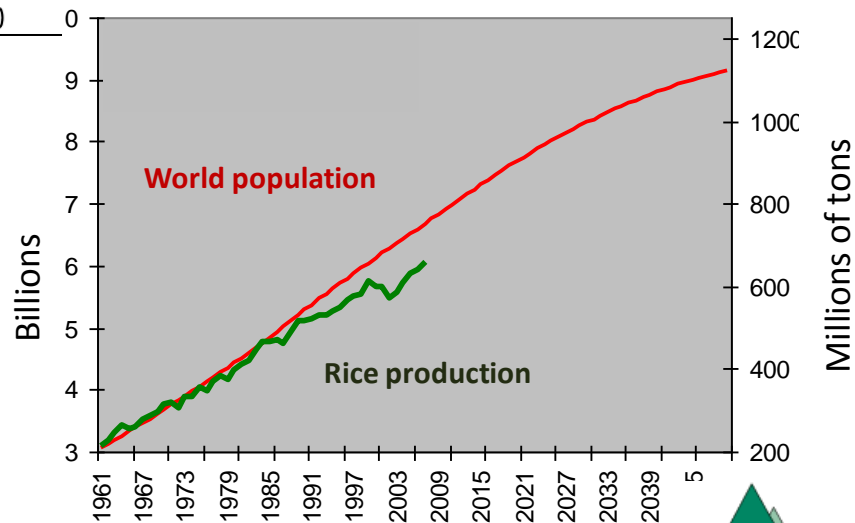


Schneising et al., ACP, 2009

Methane emission from rice
(between 7% and 19% of
global emission)

• Rice and food security

Food security has become a key global issue due to the Asian region's rapid population growth and extensive conversion of arable lands



Location of the Semarang test site in Indonesia. Cultivated areas within the region are used by rice farmers typically 7000 to 20000 m² within a flood plain. The main rice variety (IR64) has a short growth cycle (115-120 days). Production within the area can be classified into two categories:

- irrigated season where water is supplied artificially and one, two or even more rice crops per year are produced, depending on the area in some regions the crops are a two-year period (see comments)
- dry-fed season where fields irrigated by natural and in some cases with additional run-off collection provide one rice crop per year together with a secondary crop such as vegetables.



Examples of Space-Based Applications

between Scot Conzel and CESBIO in France, and the Agency for Technology



Location of the second test site, at Akita in Japan, where fields were gathered in the framework of a rice crop monitoring experiment carried out in 1992 and 1993. The targeted rice field is about 300 m long by 1 km wide, divided into 20 sub-sections of 140 m by 90 m. The rice variety grown, which is adapted to the site's relatively high latitude, has a comparatively long growth cycle of 150 days. The experiment was carried out during the entire rice growth cycle, from 1 km on October 1992 and 1993, during the 35-day ripening cycle of ERS-1.

Results of the classification of rice fields. Non-rice-vegetation has been performed using a threshold of 3 dB, which was identified as being the optimal value given the constraints in terms of test-site conditions and available SAR data. In addition to the rice/non-rice classification, the rice fields could be separated into early and late varieties, depending on the ratio value. For late varieties, the rice had not been harvested leading to an increase in backscatter between the two image acquisitions and a negative ratio in dB. For early varieties, the rice had been harvested following resulting in a drop in backscatter and a positive ratio in dB. Rice fields at the end of the cycle corresponding to late rice crops are shown in dark blue, whereas rice fields that were at the end of the cycle when the first image was acquired and are at the beginning of the cycle for the second are visualized in magenta. Rice-rice areas are shown in light green. Ground surveys confirmed that all the sites at which rice parameters were measured were correctly identified as rice crops by the method. The calculation of rice coverage is then possible from the classification.

A distinct advantage of using the ratio of backscatter values to detect changes in SAR images is that the radiometric effects due to relief are removed. This is important since the precise digital elevation models needed in order to correct for the effects of sloping terrain (terrain geocoding) are often not available in such regions.

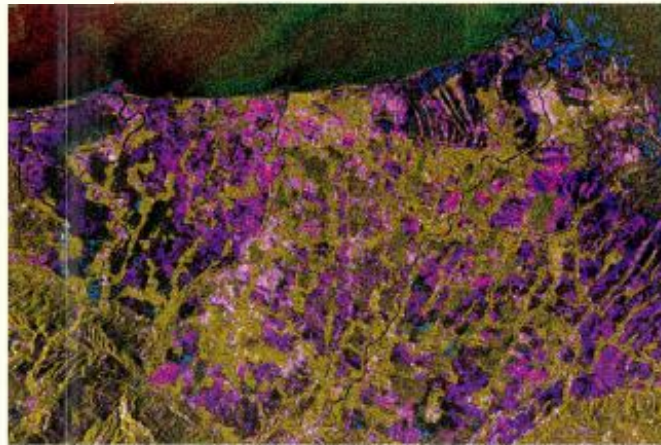
RICE MAPPING AND MONITORING

Agriculture which is responsible for providing rice-coverage statistics for the Government

A project entitled Satellite Assessment of Rice in Indonesia (SARI) was therefore set up with the objective of providing accurate and timely acreage measurements on an operational basis using ERS SAR data. To this end, a high degree of involvement of the relevant Indonesian authorities was necessary and various training programmes were conducted alongside the investigation of the infrastructure required for the task. An additional consideration was the use of standard computer hardware and image-processing software products in order to simplify the implementation of the system as an in-house service operated by the Ministry. The SARI project was initiated, with European Union support, early in 1997. However, back in 1994 a so-called Phase-1 of the project had already been conducted as a cooperative enterprise

mapping and rice-monitoring method.

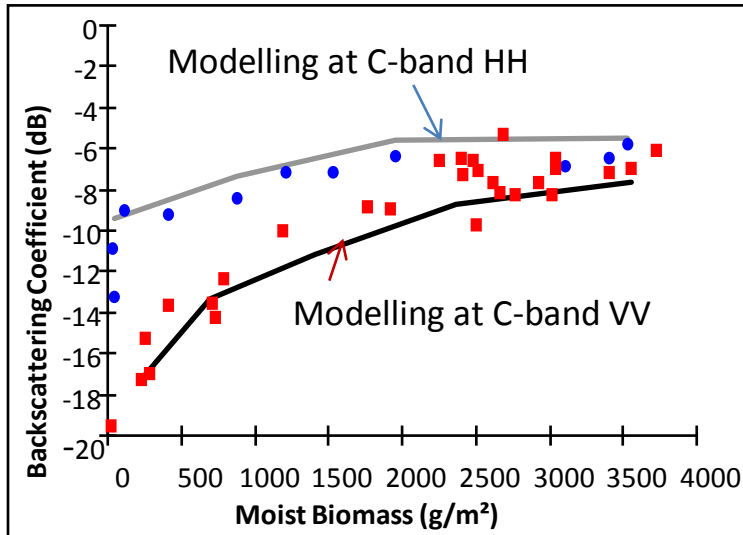
A rice-mapping method has been established that is based on the temporal change of the backscatter - the so-called change index - at the field scale. The value of this change index depends on the points during the growing cycle at which the SAR data are acquired, i.e. whether the change is over the growing season when the backscatter is increasing, or between harvesting and the beginning of the next cycle when the backscatter is decreasing. In order to apply this method, these changes need to be accurately quantified. This is made difficult because of speckle, a well-known effect in SAR imagery that gives a noisy aspect to images and introduces errors in the measurements of the backscatter. A rice-field mapping algorithm has therefore been developed that enables one to reduce speckle, derive a suitable change index, and finally separate rice and non-rice areas.



and in Thailand, Malaysia, India, Vietnam, China ...:
Rice mapping and yield estimation at local and regional scales

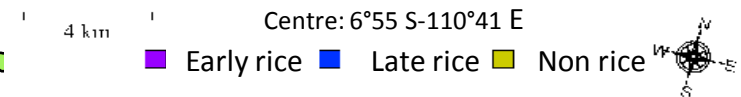
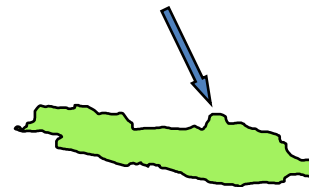
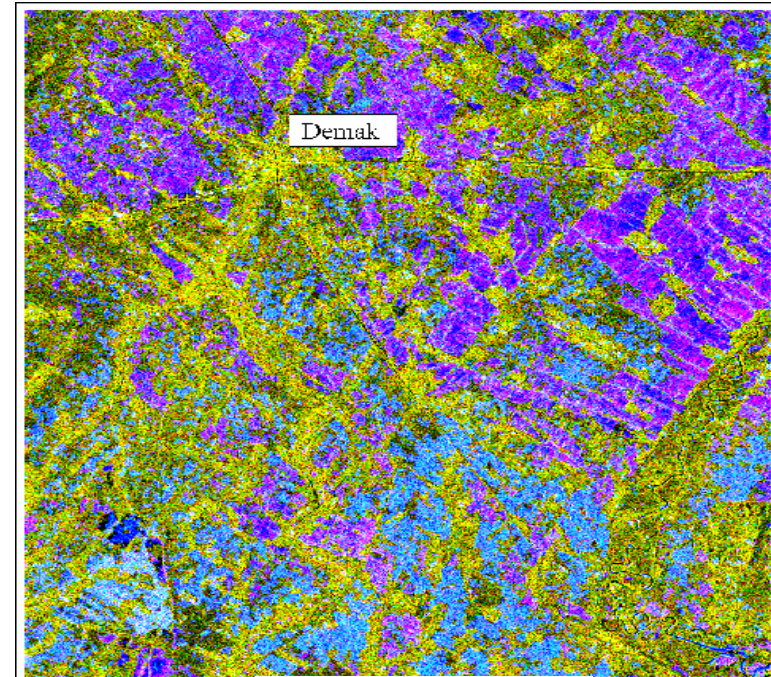


C-band SAR for rice



Rice Crop Mapping and Monitoring Using ERS-1 Data Based on Experiment and Modeling Results

Thuy Le Toan, Florence Ribbes, Li-Fang Wang, Nicolas Floury, Kung-Hau Ding, Jim Au Kong, Masaharu Fujita, *Senior Member, IEEE*, and Takashi Kurosu

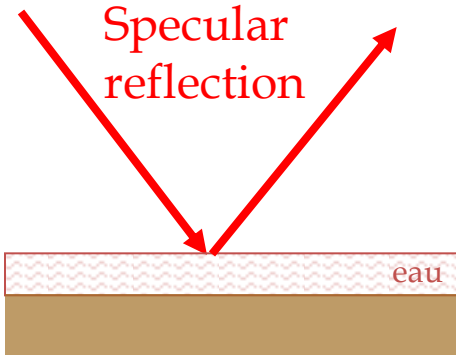


Map of rice fields derived from multitemporal ERS-1 data
Region of Semarang, Java, Indonesia

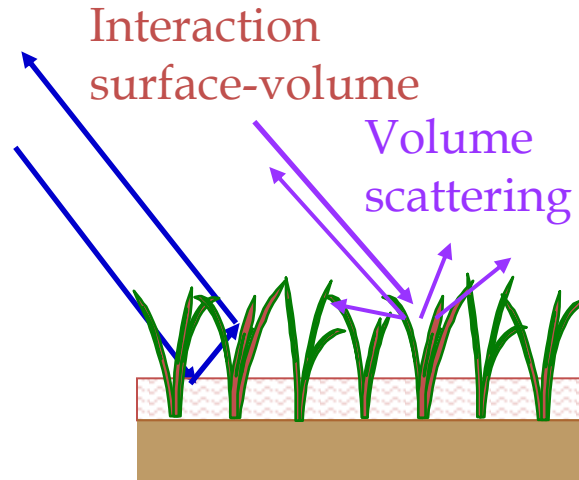


Physical interaction mechanisms

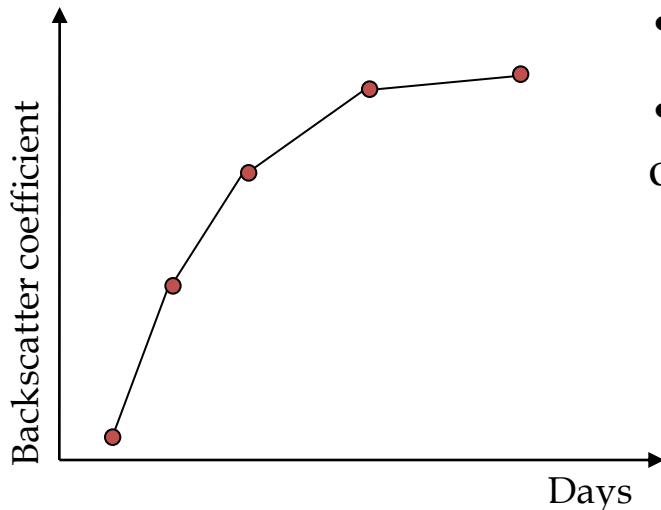
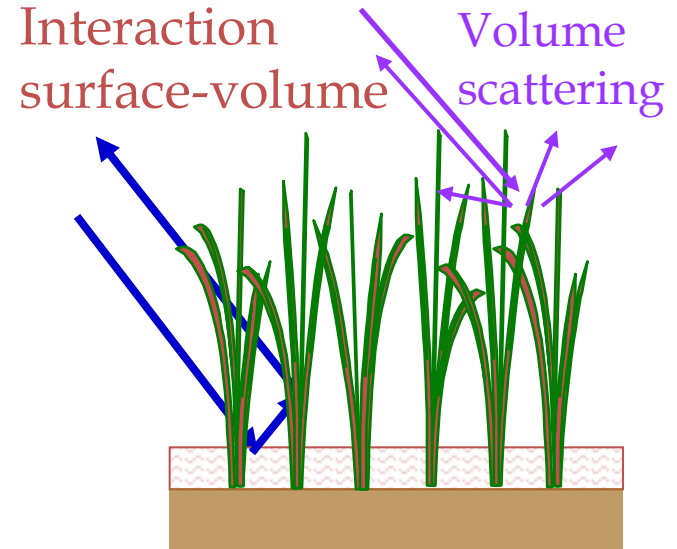
Flooded field



Early growth stage



Fully growth stage



- HH et VV increase with time
- HH/VV increases with the growth of rice because of the attenuation by vertical stems

Rice mapping using:

- HH or VV temporal change and/or
- polarisation ratio HH/VV



HH



VV

ENVISAT ASAR dual polarisation images





Rice mapping
using HH/VV

from
ENVISAT ASAR
dual polarisation images

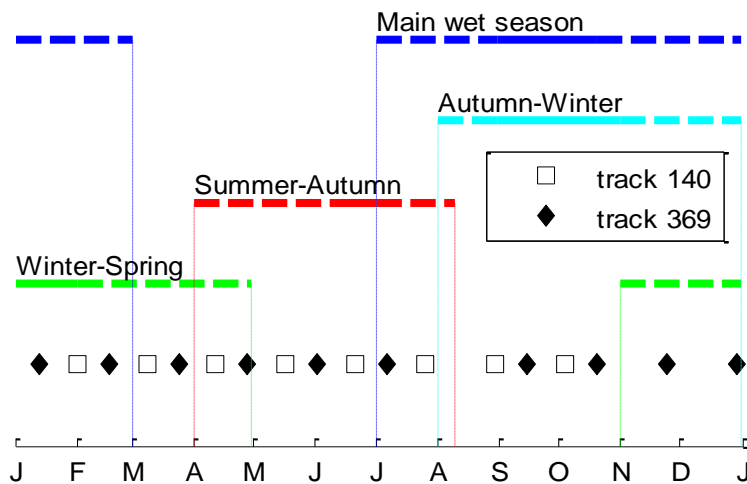
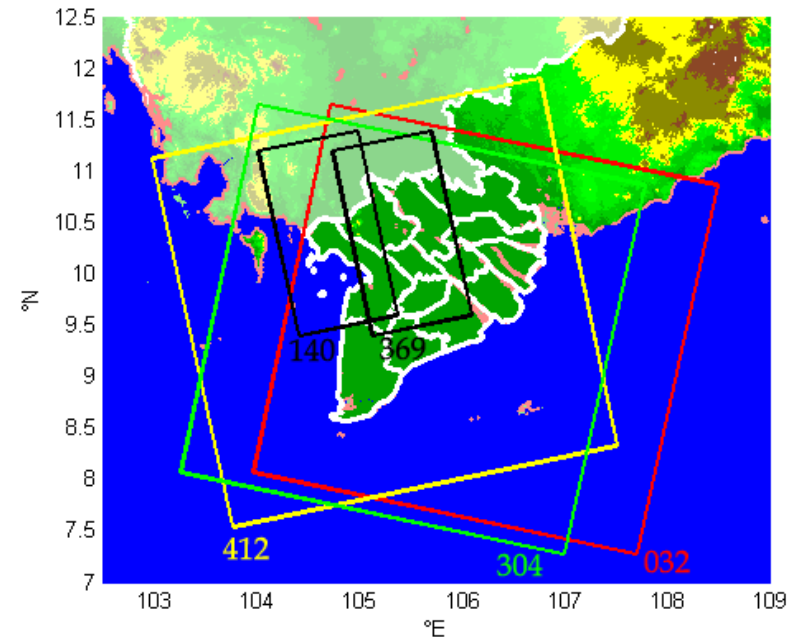
Hongze(Jiangsu)

2004 09 06

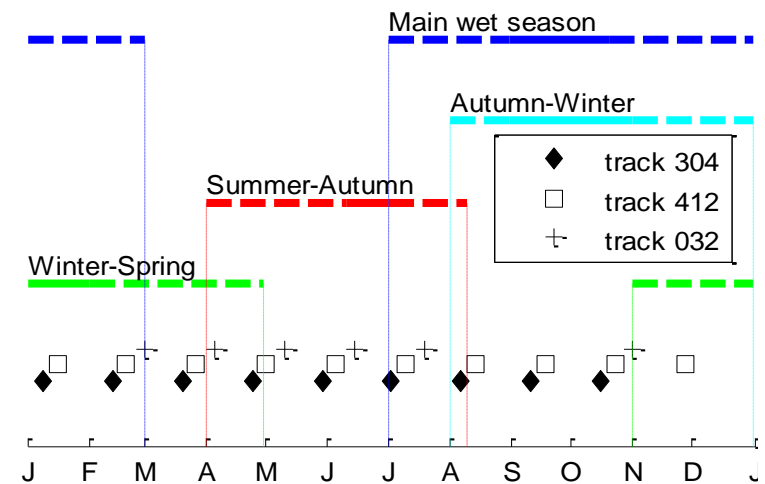


ENVISAT ASAR

	APP	WSM
Polarisations	HH et VV	HH
Pixel size	12,5m	75m
Swathy width	105 km	405 km
incidence angle	19,2°-26,7°	17°-42°
Number of looksrange	1	7
Number of looks azimuth	2	3

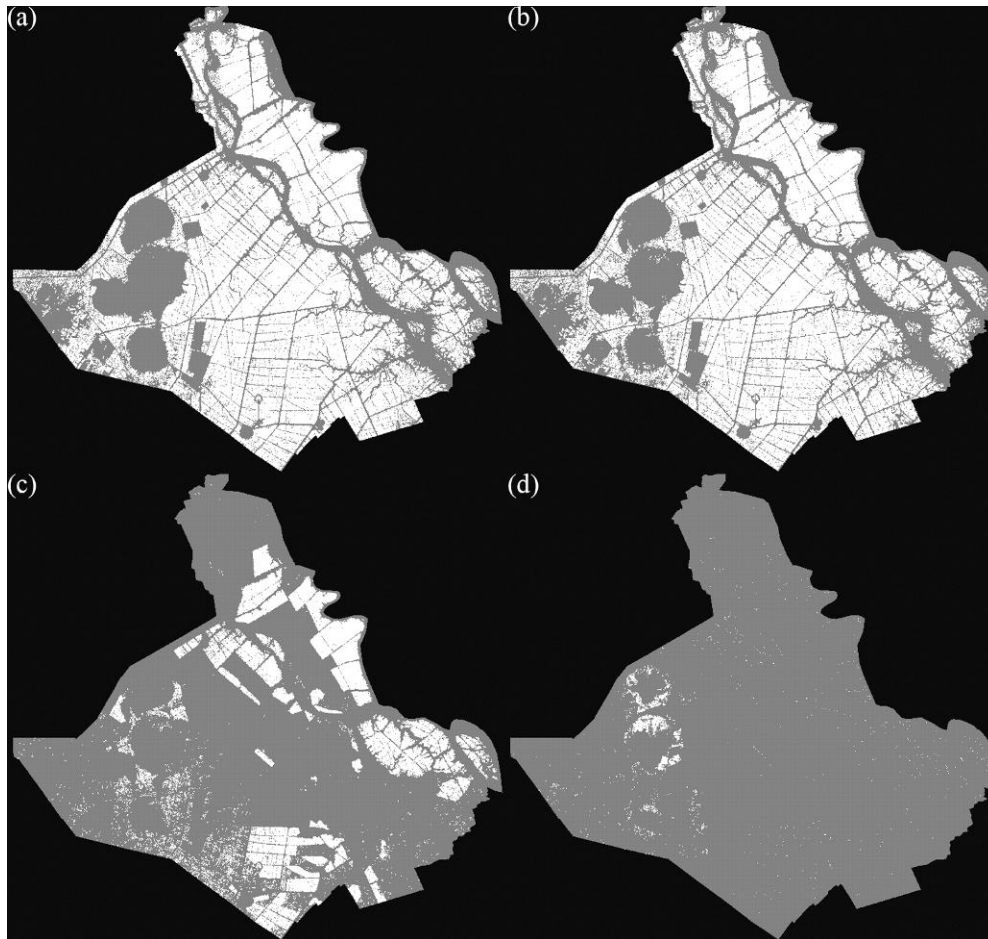


APP- use of polarisation ratio



WSM -use of temporal change

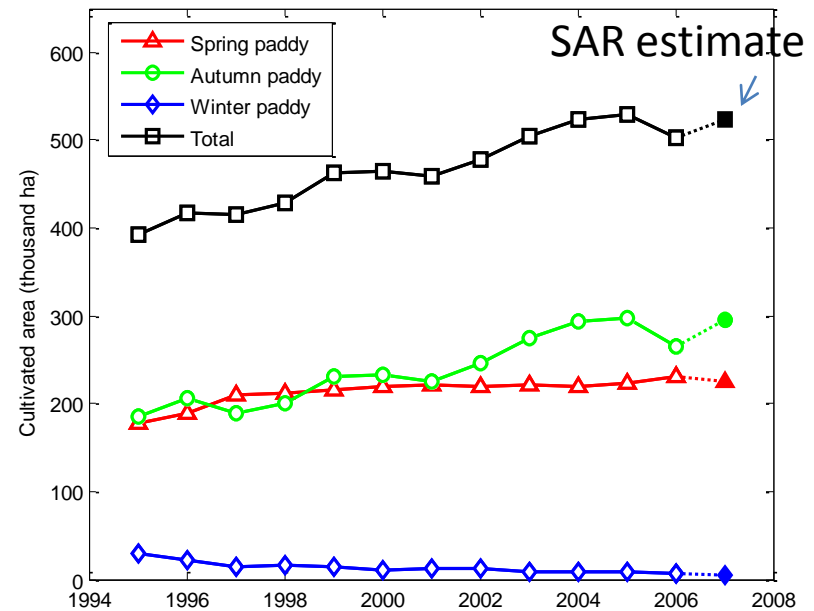
Rice mapping using polarisation ratio from ENVISAT ASAR dual polarisation images



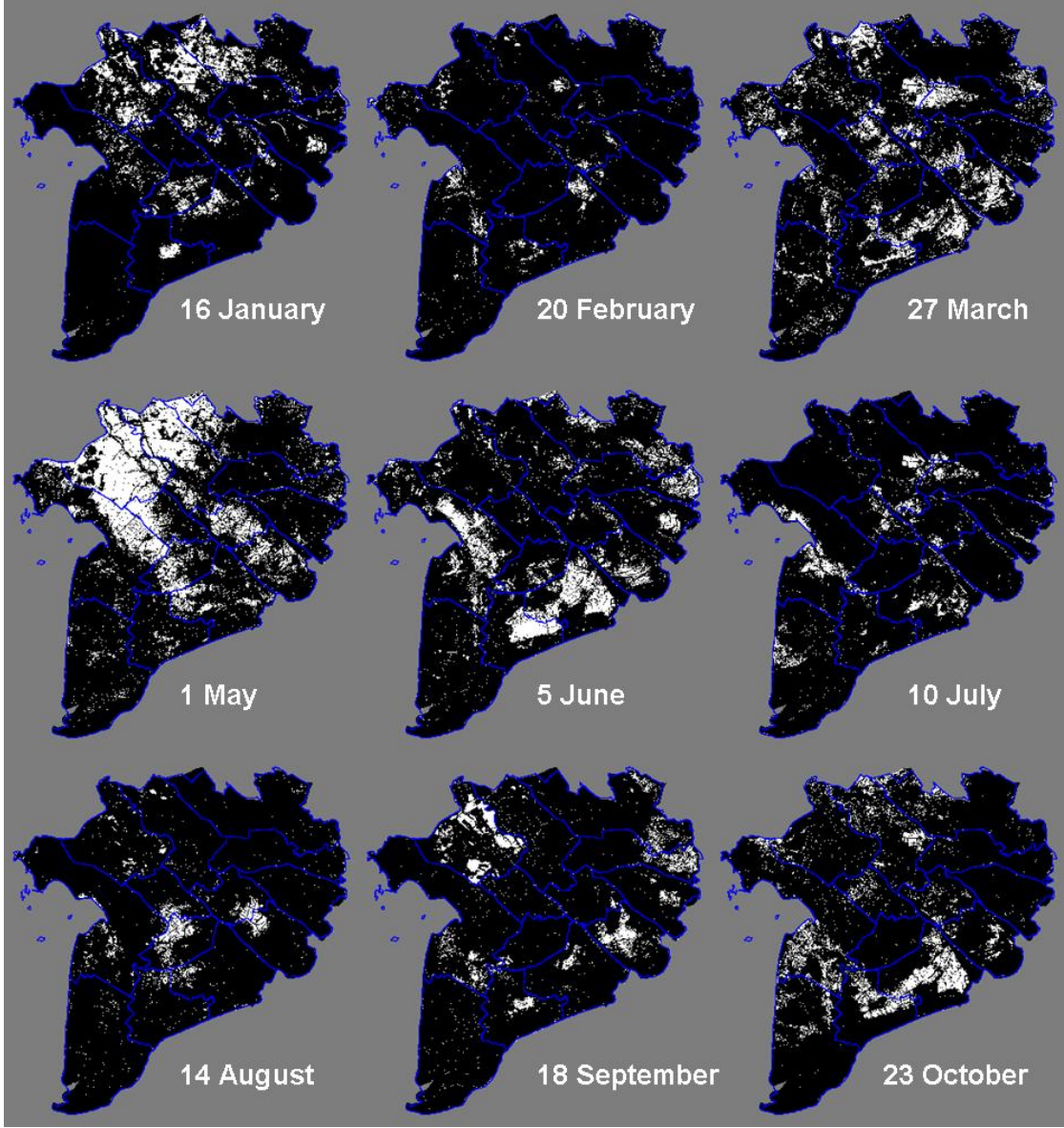
Province of An Giang, Vietnam

Bouvet et al, 2008

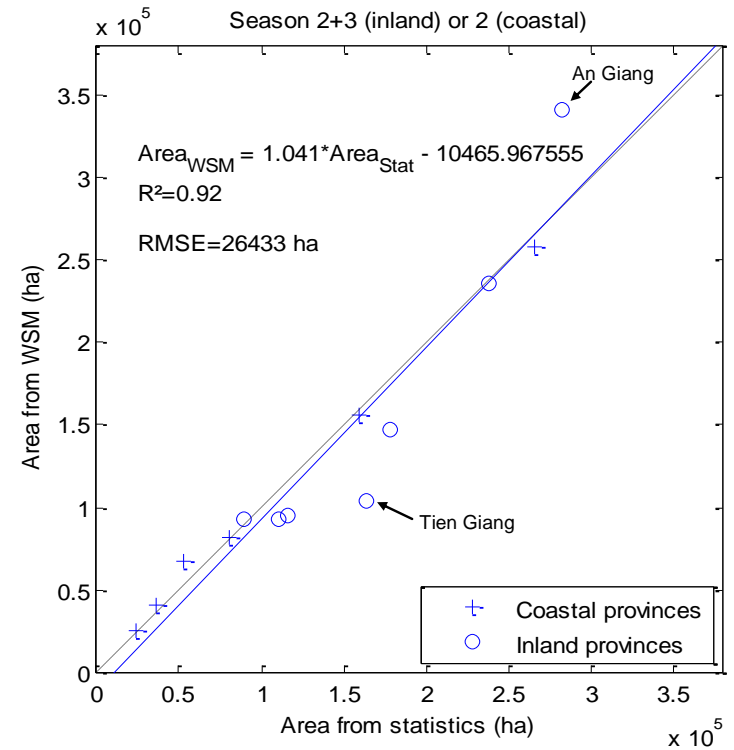
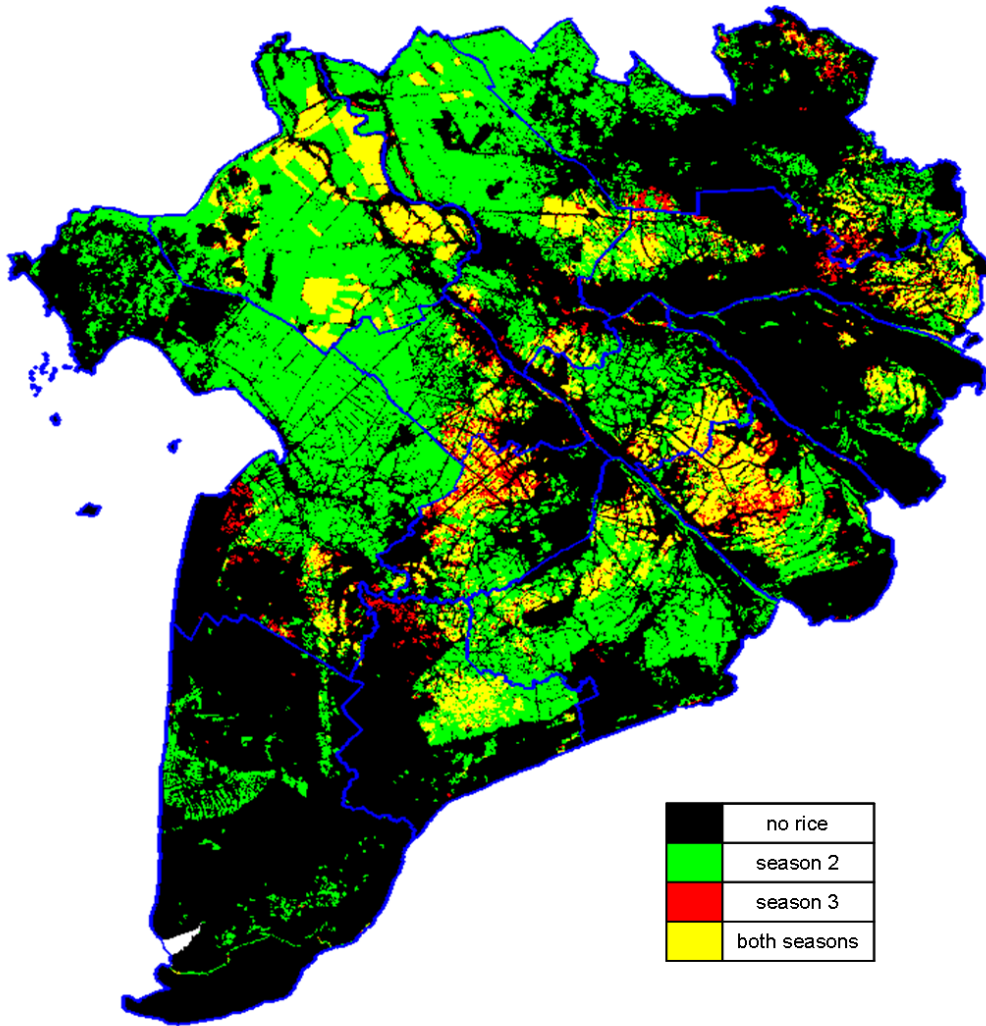
Rice area (1000'ha)	Rice season 1	Rice season 2	Rice season 3
SAR	224,3	294,8	5
Vietnam Statistics	230,6	282,7	7,3
Difference	-6,3	12,1	-2,3
Difference in %	-2,7%	4,3%	-31,5%



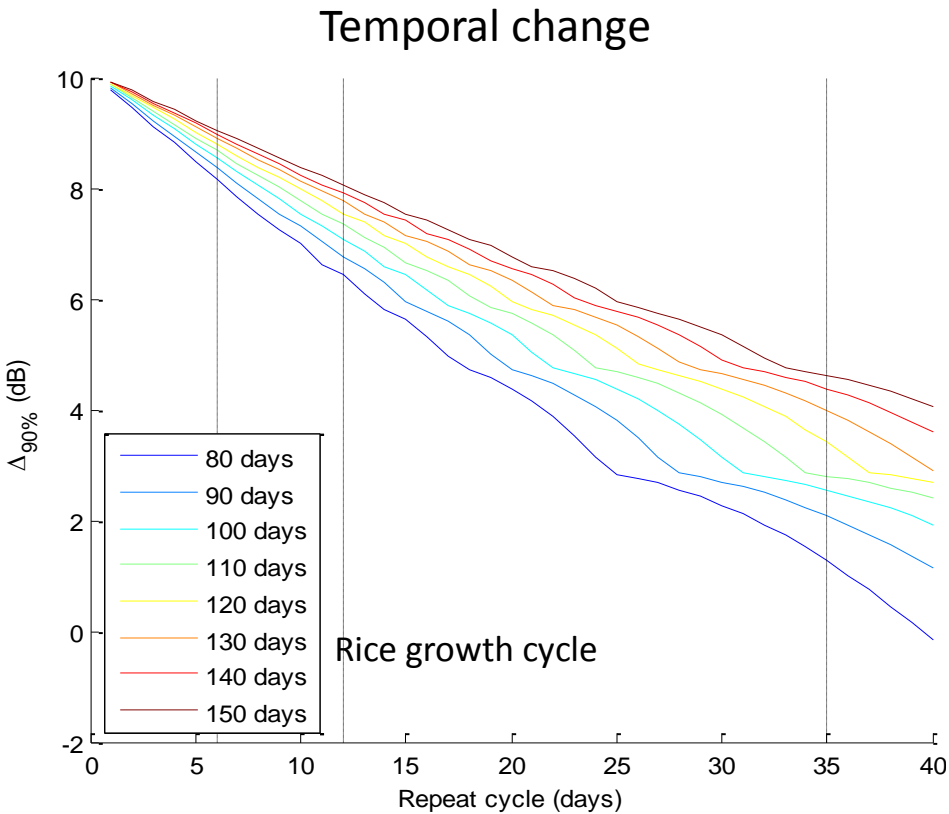
Rice map using ASAR multitemporal WSM data



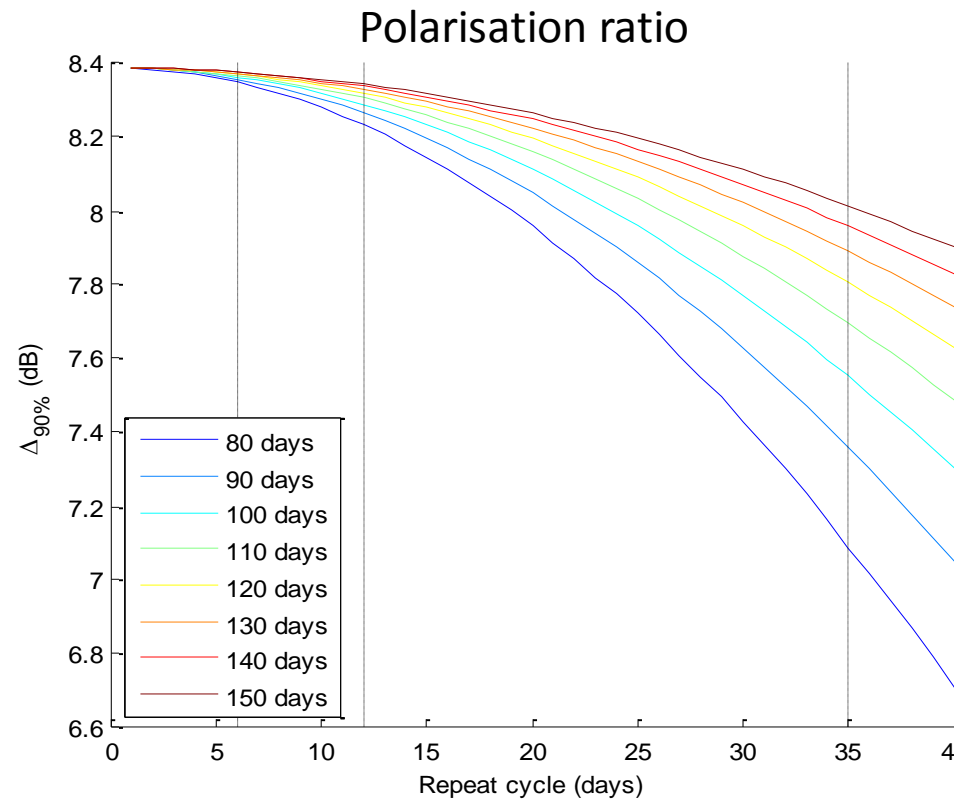
Rice map of South Vietnam



Temporal change and polarisation ratio as a function of rice growth cycle and repeat cycle



Sentinel



ASAR

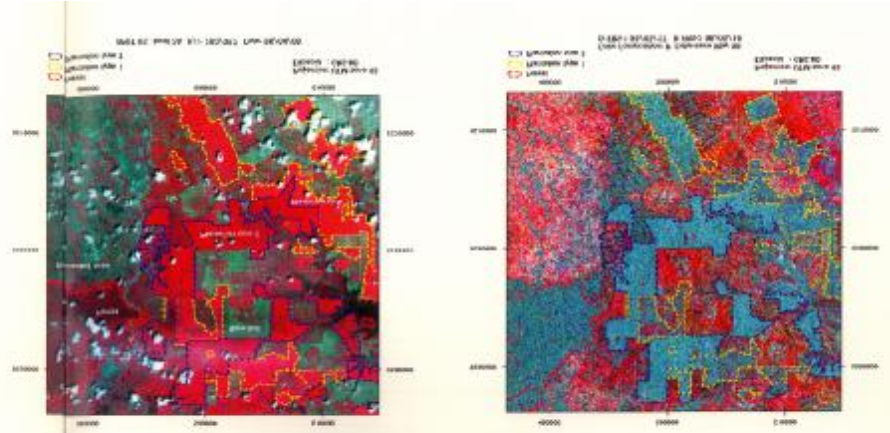
Forest monitoring



Multitemporal SAR methods for deforestation monitoring

re-composition dates based on their
in addition, the identification of different
deforestation features are closely related
to the in which the deforestation is based on
the above figure shows an ERS-1 SAR

was and one during the dry season/
seasons each year, one during the
seasoned period (the two ERS-1 SAR
deforestation monitoring can be
obvious because, which means that



CESBIO, and also the JRC TREES projects

information. The degree of confidence
low. It may be a discrimination of
confidence - compared with the
confidence. The information
based on the two SAR images
data acquisition from two satellite images
temporal information needed. ERS-1 SAR
images to identify deforestation
non-forest areas and forest
area is likely to be used for
deforestation monitoring in tropical
regions.

temporal information needed. ERS-1 SAR
images to identify deforestation
non-forest areas and forest
area is likely to be used for
deforestation monitoring in tropical
regions.

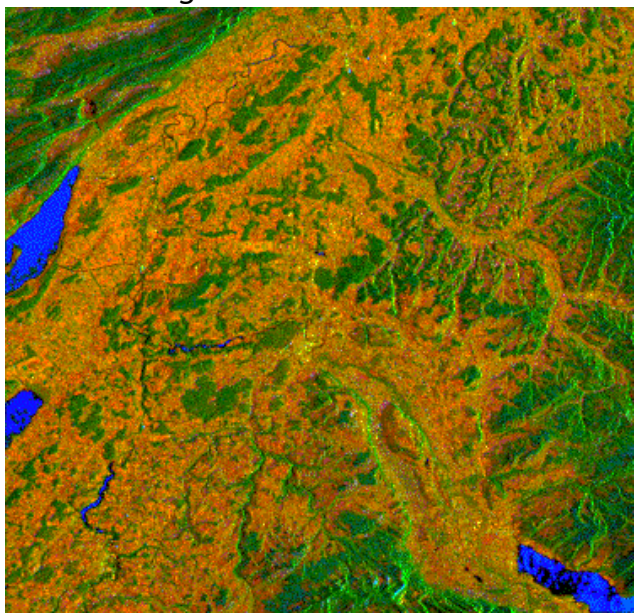
TROPICAL FOREST MONITORING



Interferometry for forest mapping and parameter retrieval

Forest mapping

Wegmueller et al 1996



Bern (CH), ERS-1, 24/27 Nov. 1991:
 RGB composite of interferometric correlation (red), backscatter intensity (green), and backscatter change (blue).

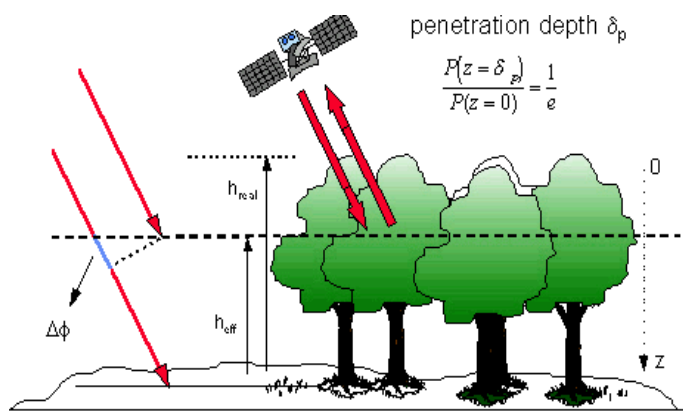
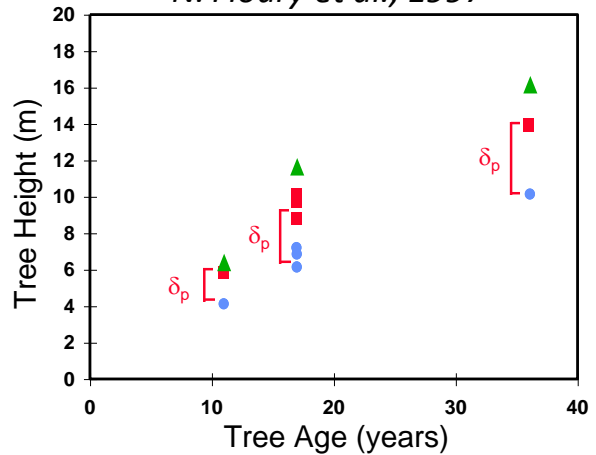


Figure 8: Determination of canopy height from interferometry

$$\frac{P(z = \delta_p)}{P(z = 0)} = \frac{1}{e}$$

Height in temperate forest

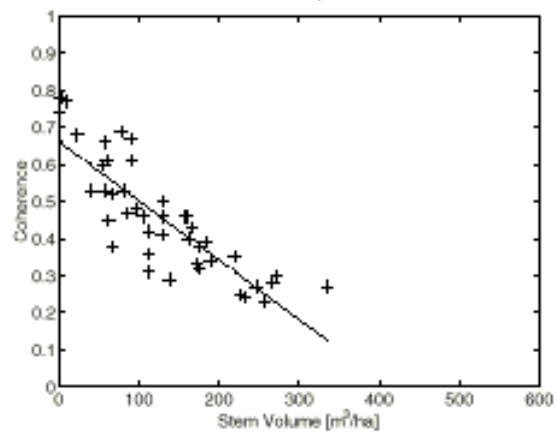
N. Floury et al., 1997



- Estimated Height from Interferometry
- Estimated Height from Interferometry + Simulated Penetration Depth (δ_p)
- ▲ Actual Height

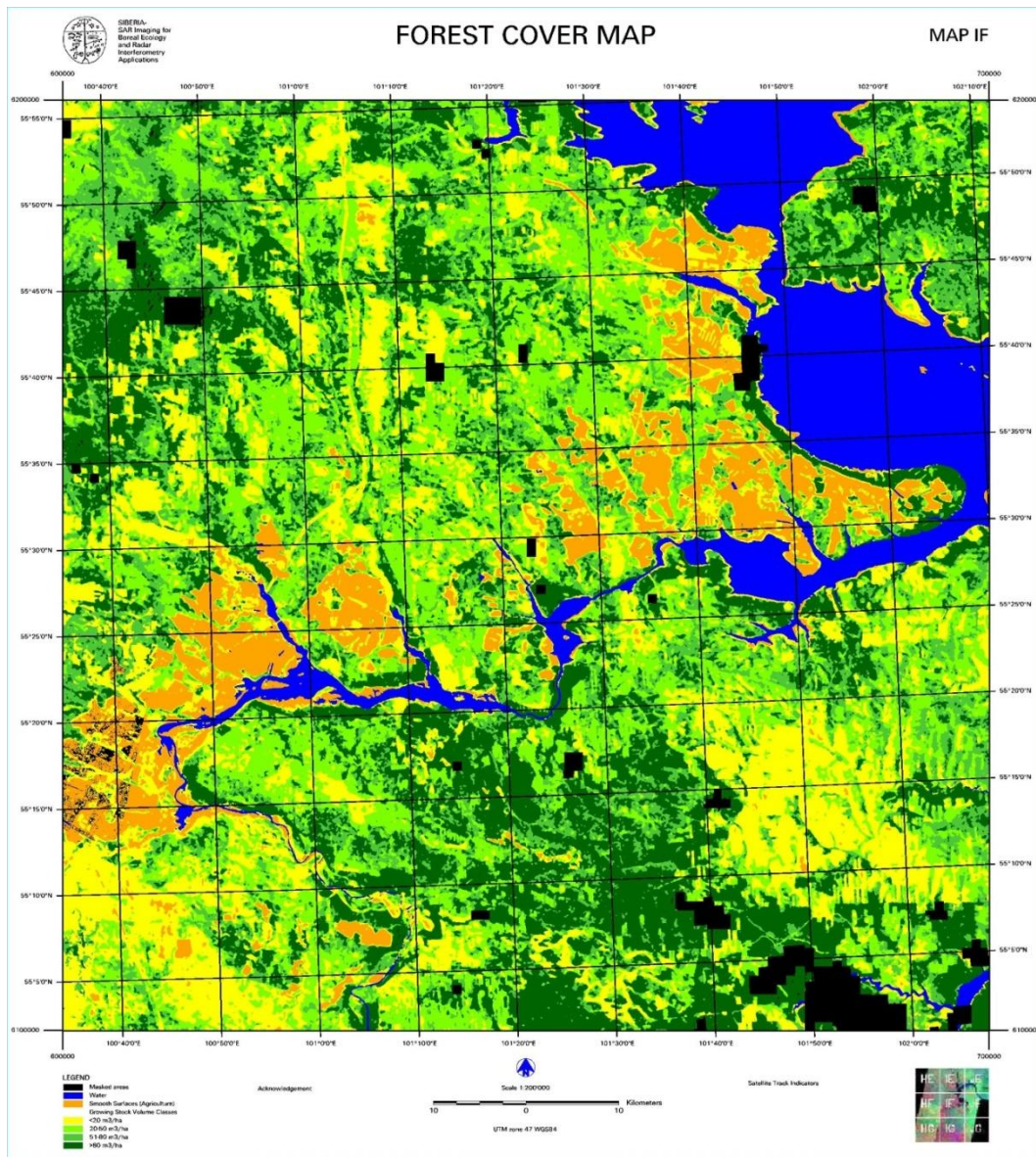
Stem volume in boreal forest

Askne et al., 1998



ERS coherence versus stem volume for Kättböle test-site. Image pair 17th/18th March 1996.



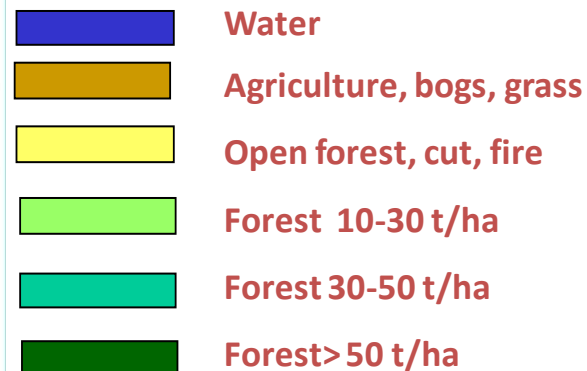


SIBERIA (SAR Imaging for Boreal Ecology and Radar Interferometry Applications), EU/CEO project no ENV4-CT97-0743.

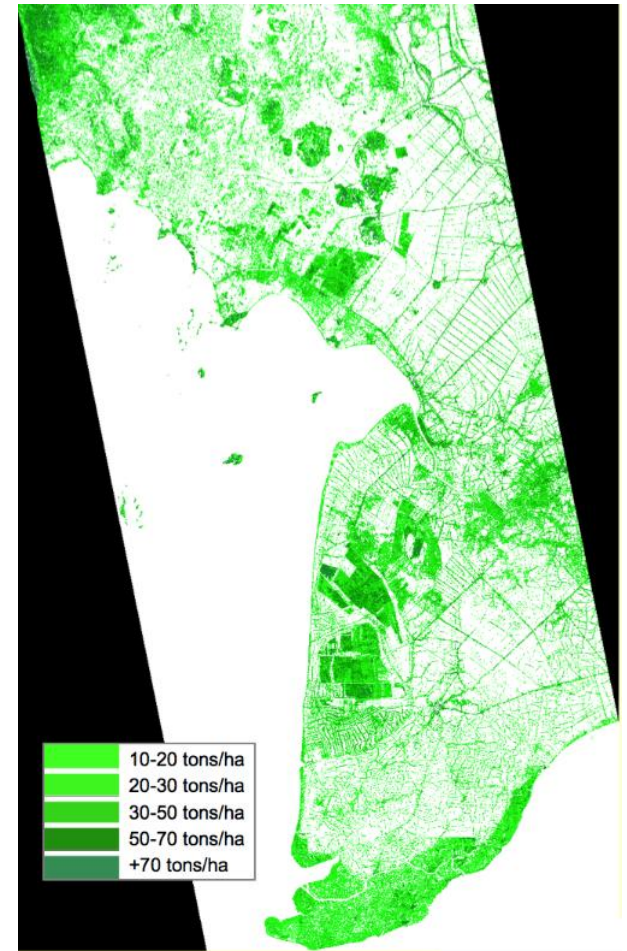
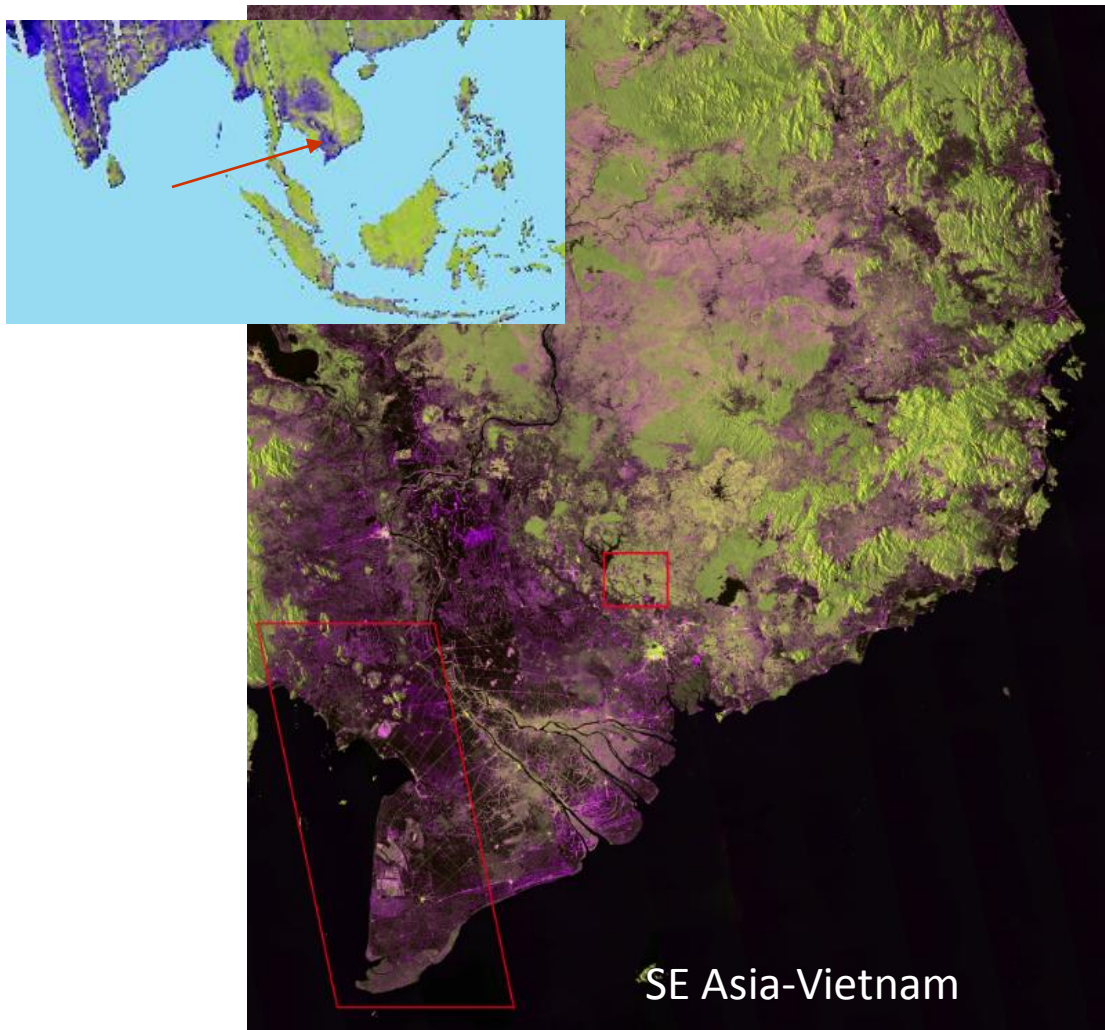
ACHIEVEMENT: Generation of a forest map of central Siberia from ERS-1/ERS-2 Tandem coverage 1997 JERS coverage 1998

RESULTS: 96 forest cover maps (100 km X 100 km) covering 650000 km². An example of map is shown on the left.

C. Schmullius



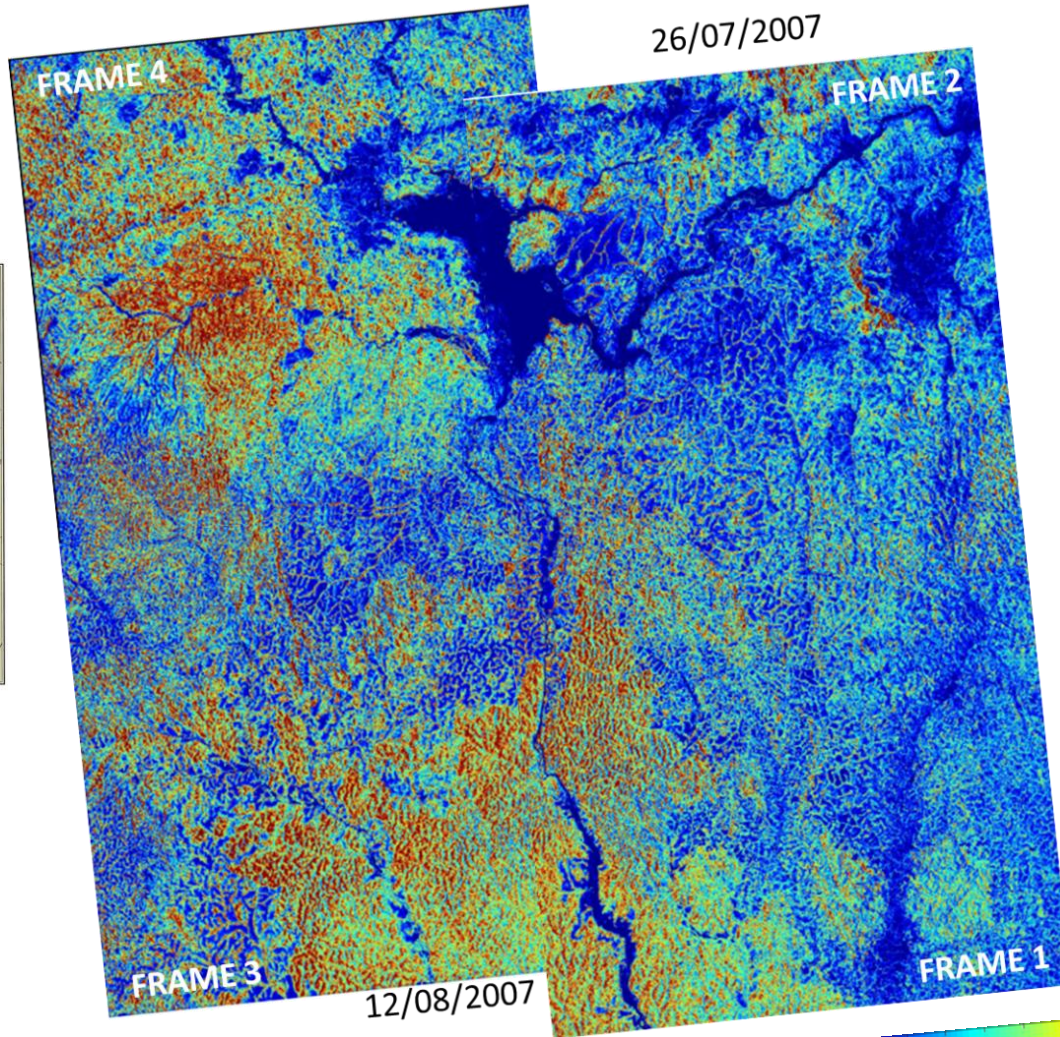
Biomass map from PALSAR: illustration



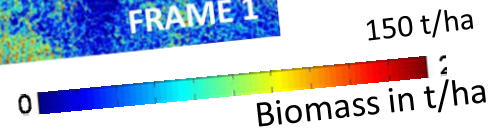
Le Toan et al., K&C Jan 2009



Forest-Savannah biomass using PALSAR

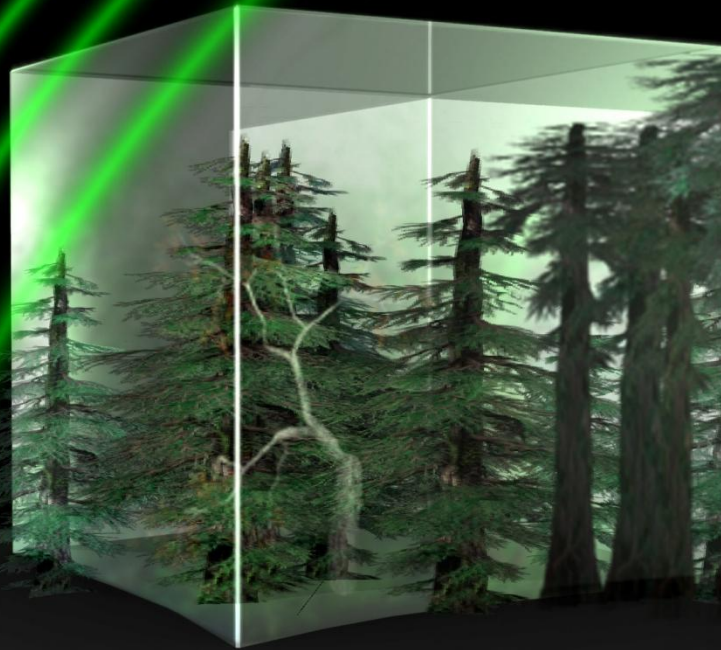


~120 km x 120 km





biomass

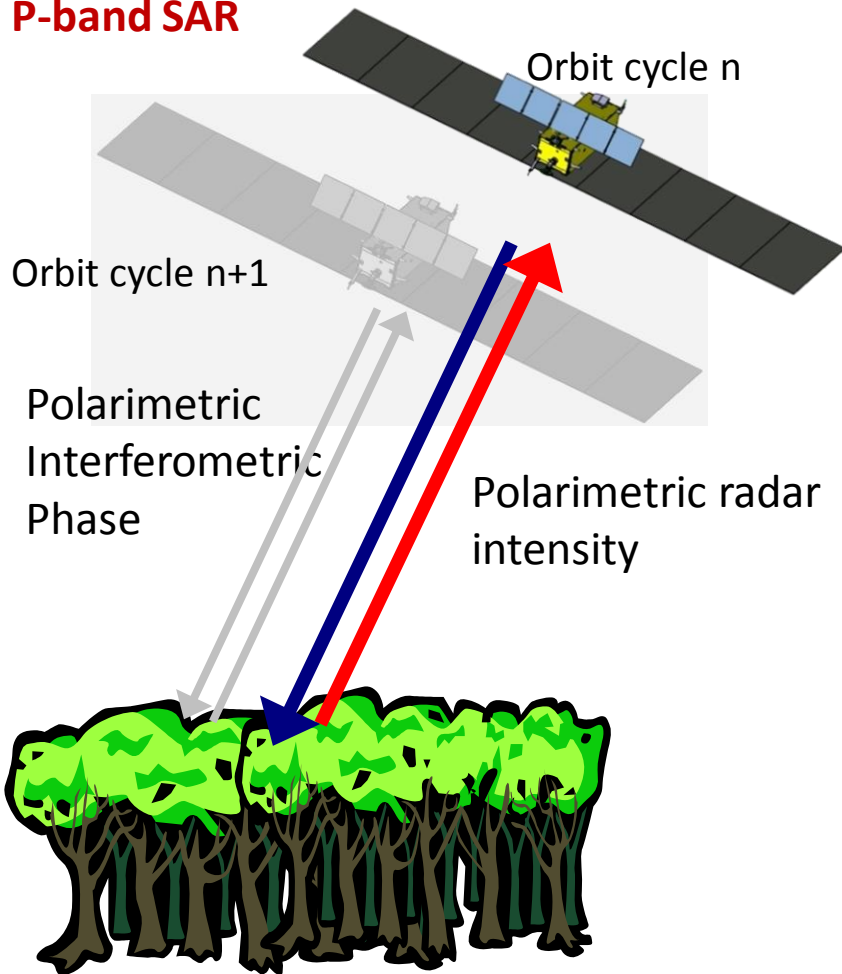


**TO OBSERVE FOREST BIOMASS
FOR A BETTER UNDERSTANDING OF THE CARBON CYCLE**

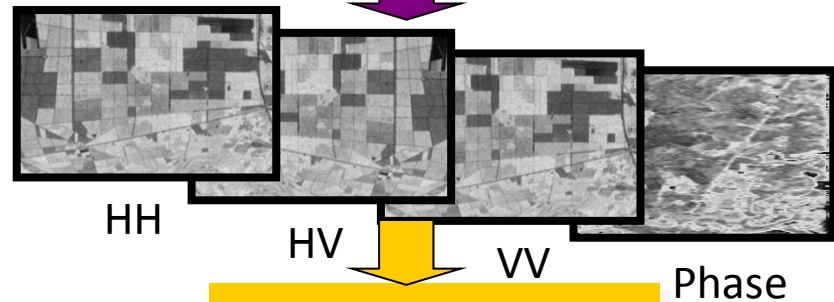


BIOMASS observation concept

P-band SAR



Calibration, Ionospheric correction

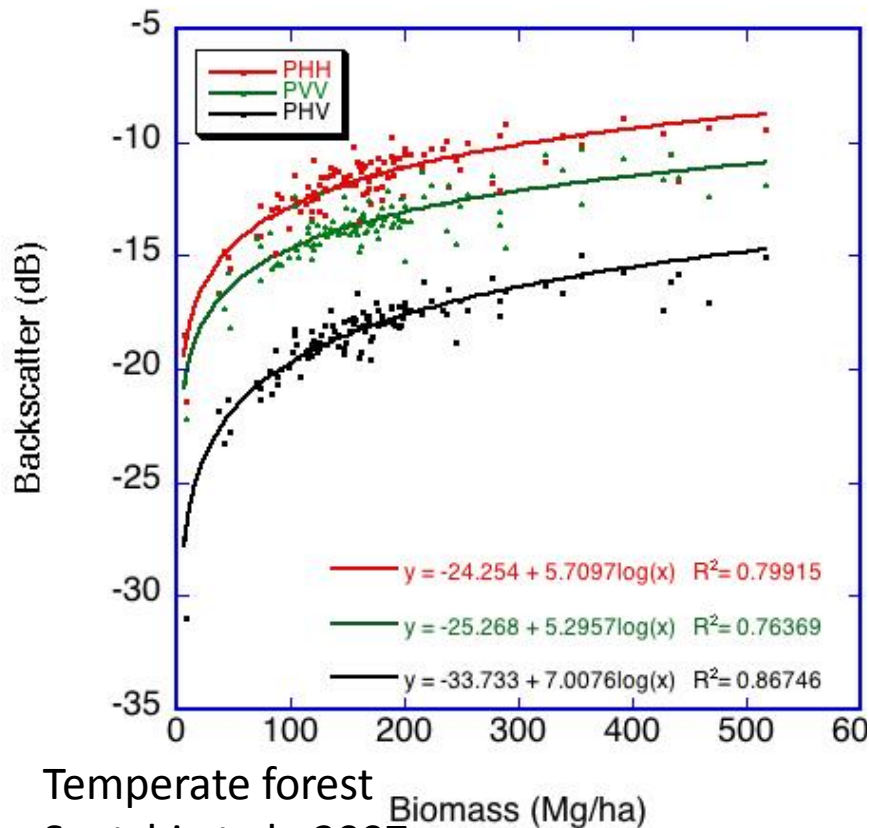


Retrieval algorithm

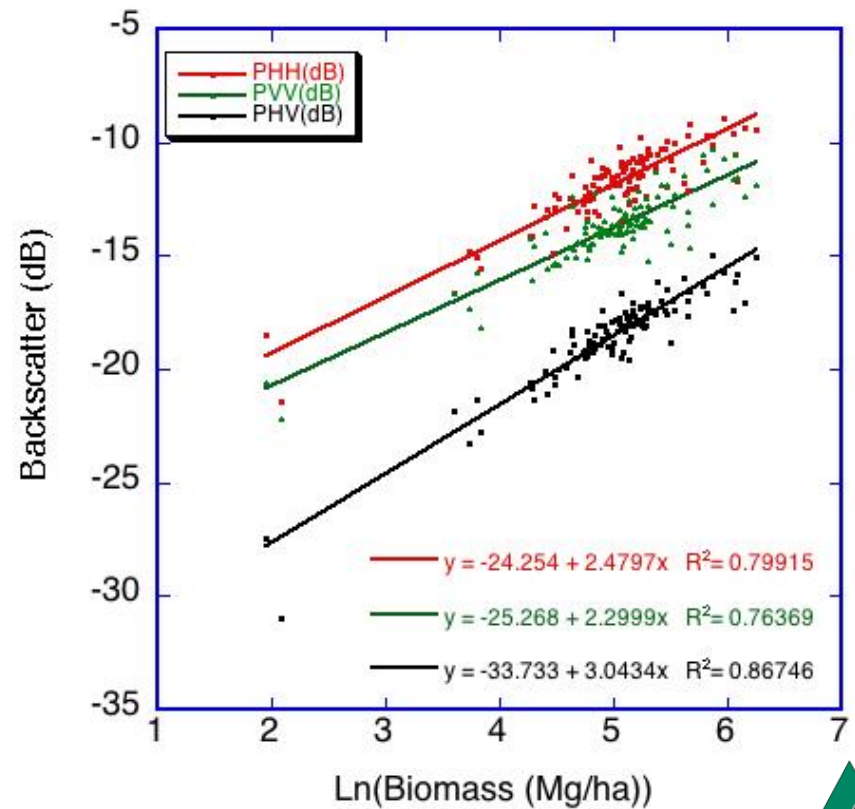
- Forest biomass
- Forest height
- Forest biomass temporal change
- Forest disturbance

Past results on P-band intensity

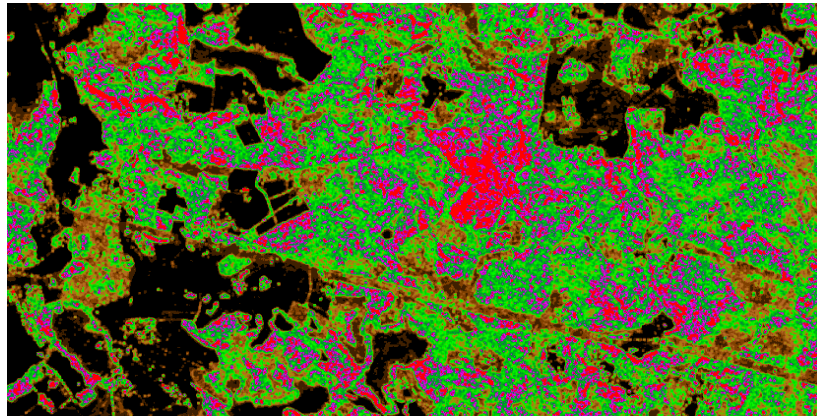
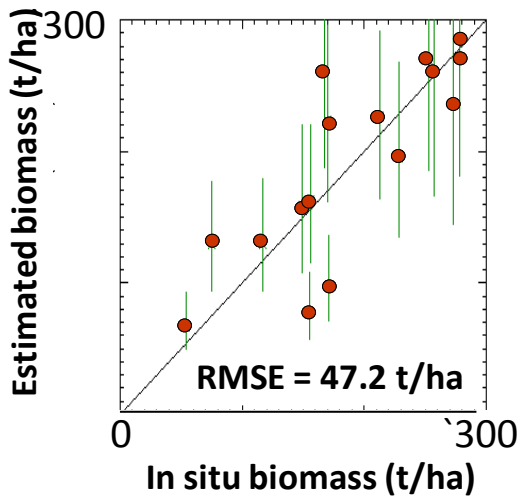
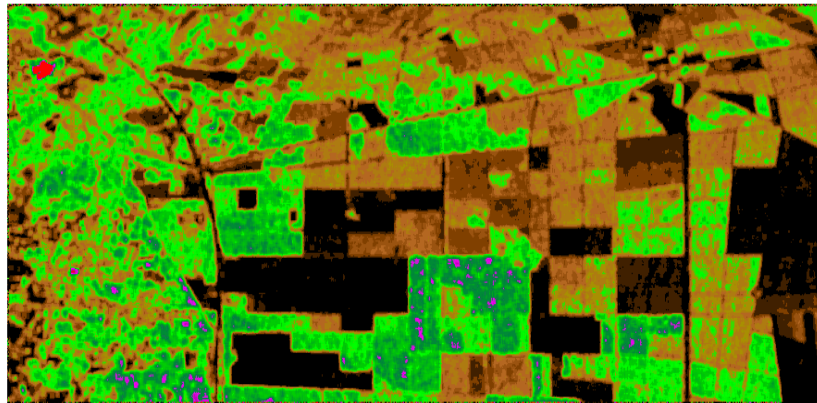
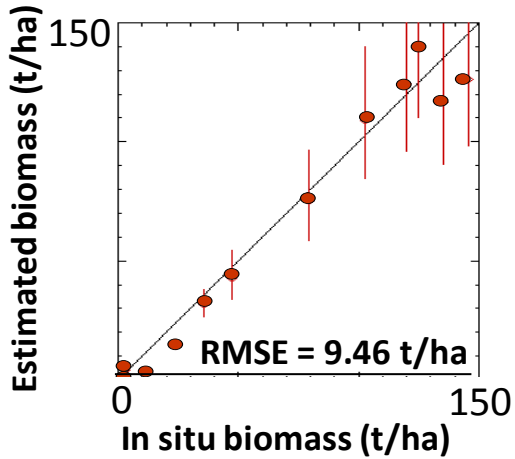
Experimental relationship between P-band Backscatter and Aboveground Biomass



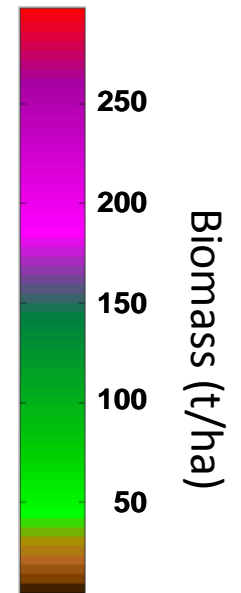
Temperate forest
Saatchi et al., 2007



Forest biomass mapping using P-band HV intensity



Les Landes



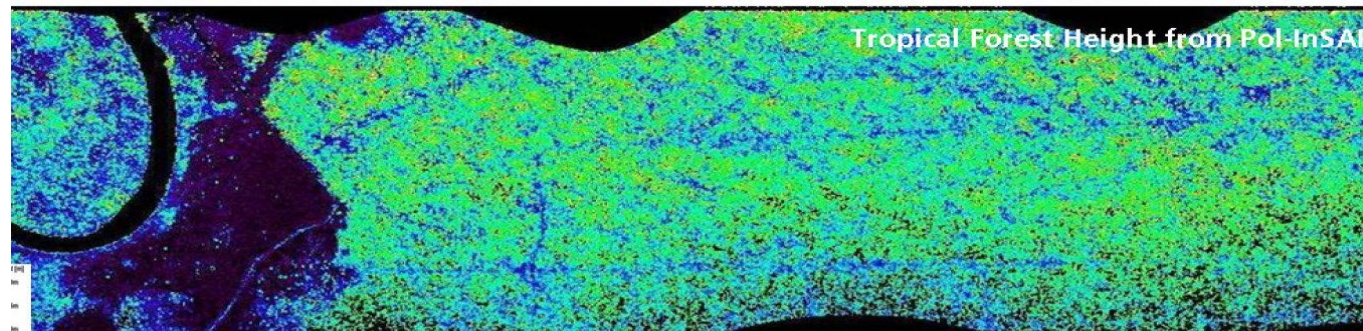
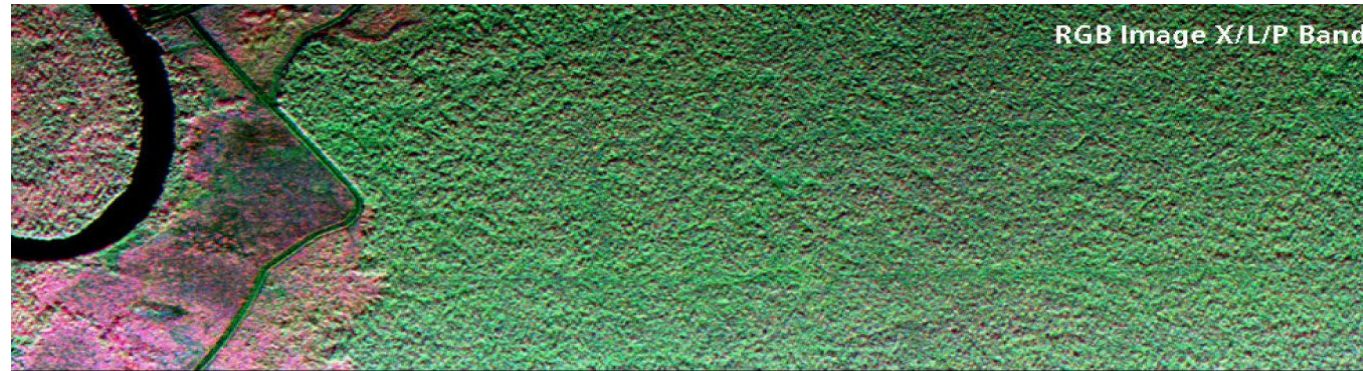
Remningstorp



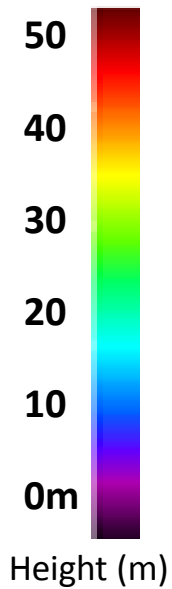
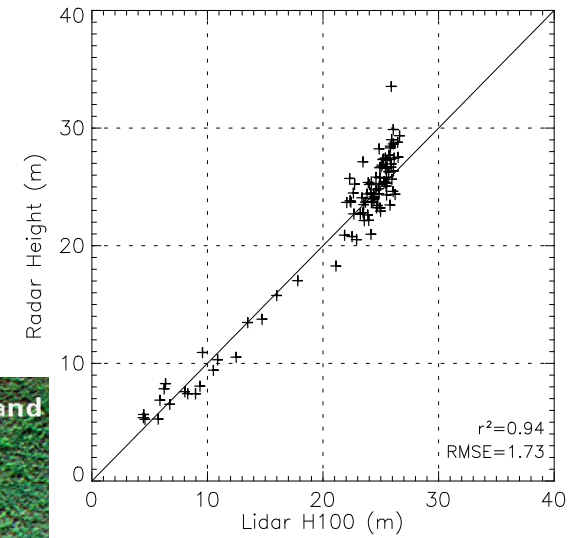
Pol-InSAR

Tree height inversion

Hajnsek et al., 2009

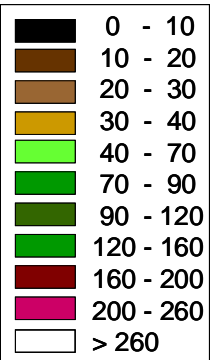
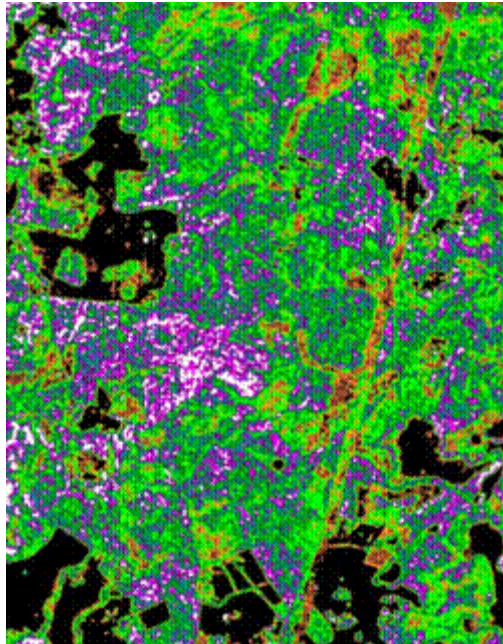


Peat Swamp forest, Mawas, Kalimantan

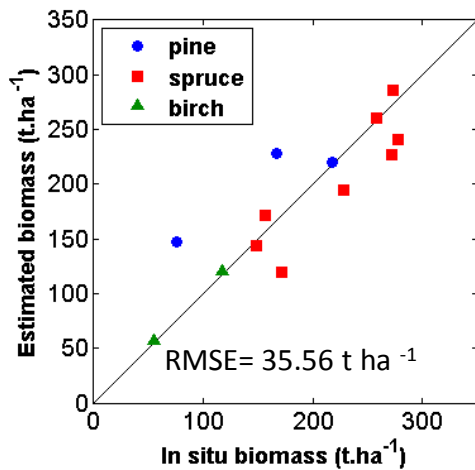


Biomass inversion combines intensity and height

Biomass from Intensity



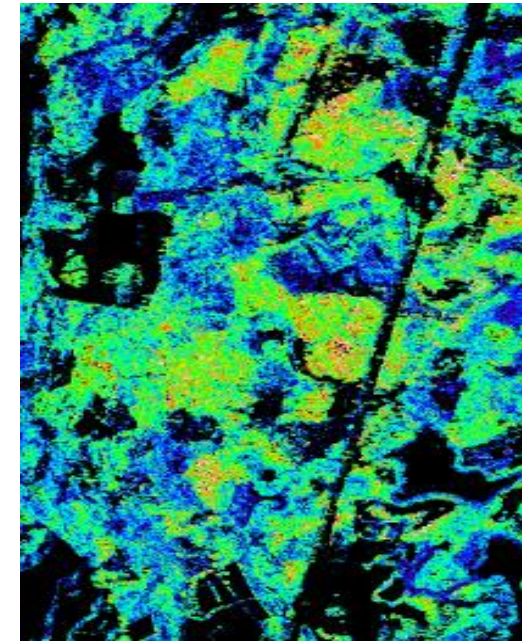
Biomass
(ton/ha)



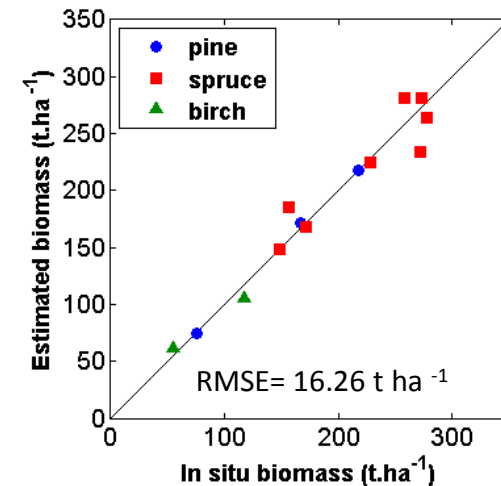
Intensity + Pol-InSAR



Pol-InSAR height



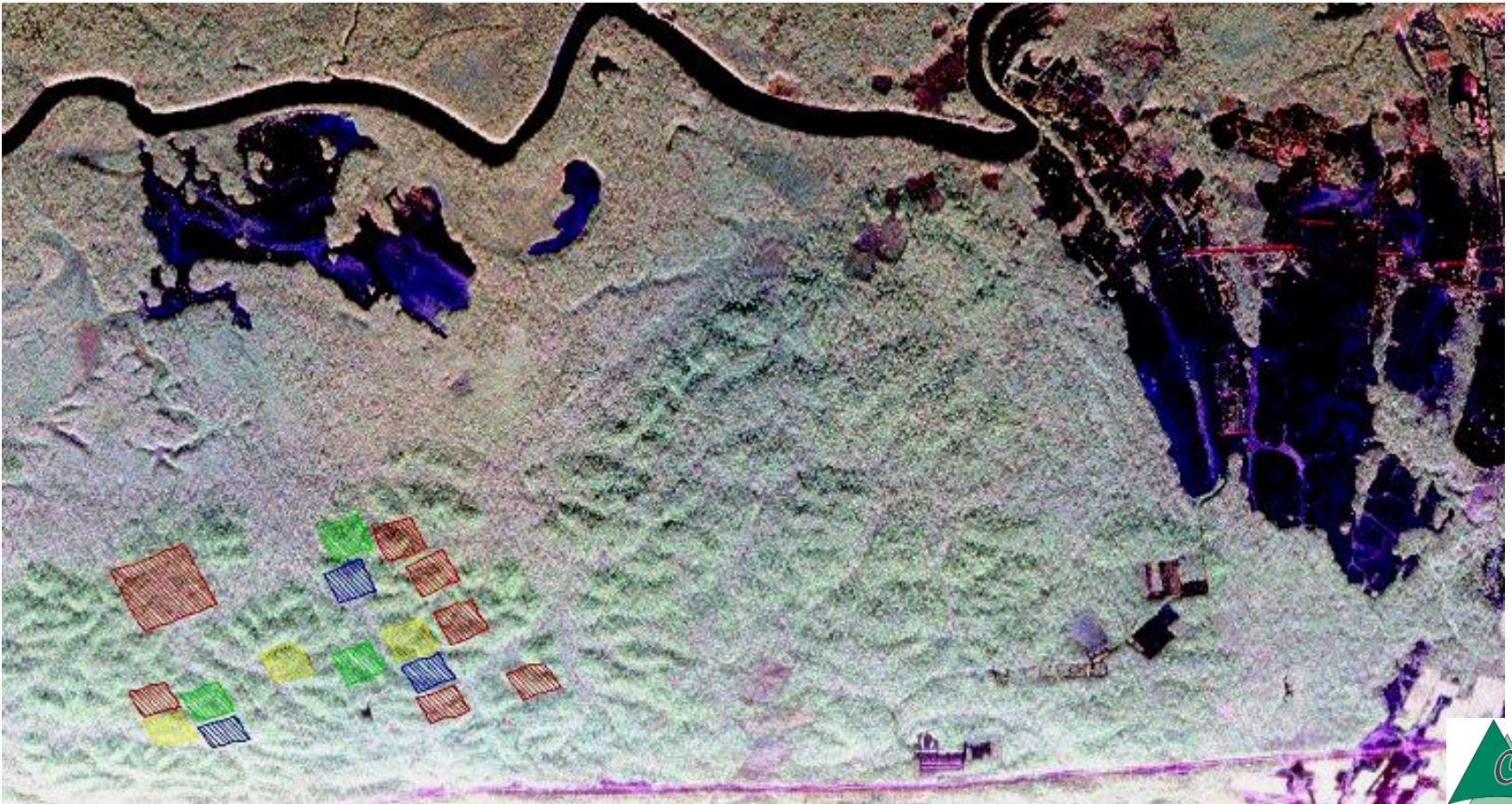
Height (m)

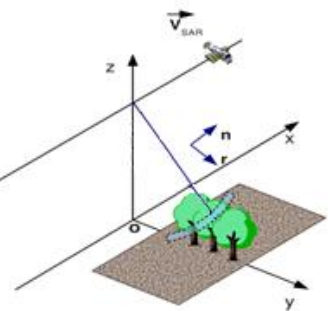


Challenging issue: to retrieve biomass > 300 ton/ha

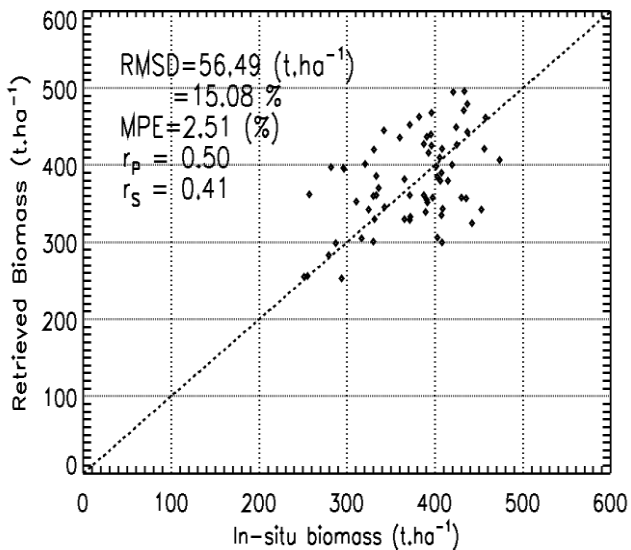
HH, VV, HV

TropiSAR P-band image, Paracou, French Guiana

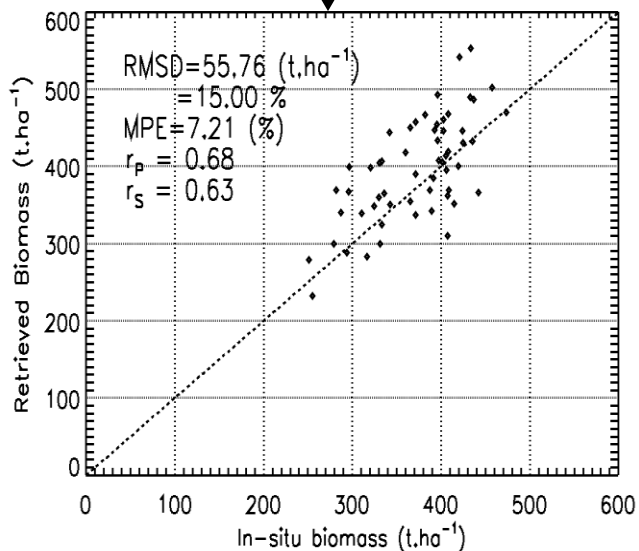
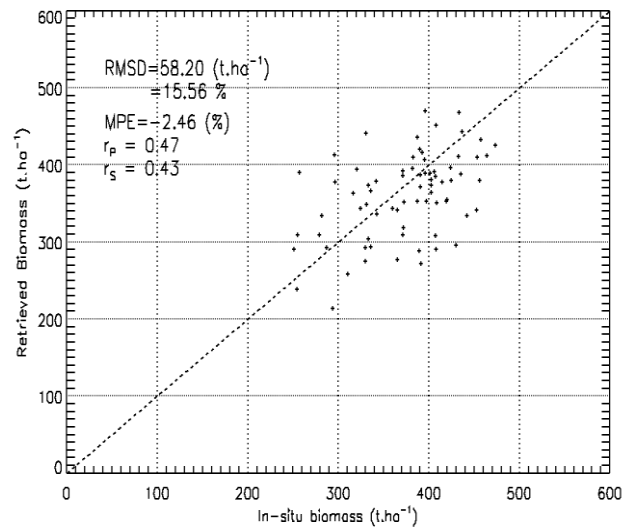
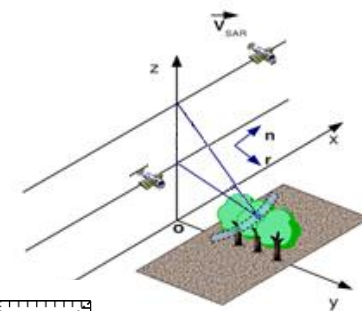




Intensity hv



PolInSAR



Inversion relying on a combination of intensity and PolInSAR